Theoretical Study of Double-Heterojunction AlGaN/GaN/InGaN/δ-doped HEMTs for Improved Transconductance Linearity

Tsung-Hsing Yu
Inforsight Computing
E-mail: thyu@inforsight-computing.com

***Abstract*—The aim of this study is to propose a novel double-heterojunction high electron mobility transistor (DH-HEMT) structure, $Al_{0.3}Ga_{0.7}N/GaN/In_{0.15}Ga_{0.85}N$/δ-doped, to improve transconductance linearity. A theoretically based quasi-two-dimensional model is well calibrated with experiments and is used to project the transistor performance. It is found that a thin $In_{0.15}Ga_{0.85}N$ back barrier and δ-doped layer significantly enhance carrier confinement and increase carrier concentration in the channel. It is the combination effect of enhanced carrier confinement and increased carrier concentration that leads to a larger voltage swing. A wider linear range of transconductance can be achieved on account of the larger voltage swing. Moreover, this novel structure not only improves the transconductance linearity but also increases its maximum transconductance and the corresponding drain current, which is beneficial to high power and high frequency applications.**

Keywords—transconductance; g_m; linearity; HEMT; double-heterojunction; InGaN; δ-doped; polarization

I. Introduction

Due to the superior material properties such as high breakdown voltage, high saturation velocity, and high thermal conductivity, III-Nitride devices are expected to offer better high frequency, high power, and high temperature performance compared to conventional Si and GaAs devices. However, GaN high electron mobility transistors (HEMTs) have been found that their transconductance g_m, current gain, and power gain drop off at high current levels [1]. To solve this issue, several methods have been presented and reported in the literature [1-4]. These are (1) distributed three-dimensional (3D) channel electrons induced by a highly scaled graded channel [1], (2) transverse electric field reduction through the use of a composition channel [2], (3) enhanced electron confinement with InGaN back barriers [3-4]. Though much progress has been made by these researchers, to the author's knowledge this is the first theoretical study of a novel structure $Al_{0.3}Ga_{0.7}N/GaN/In_{0.15}Ga_{0.85}N$/δ-doped double-heterojunction HEMT (DH-HEMT) to improve transconductance linearity.

Since polarization fields can induce a larger sheet charge and alter the band bending at the GaN/InGaN heterointerface, the carrier confinement in the DH-HEMT is significantly enhanced. Furthermore, an inserted δ-doped layer at the backside of the InGaN layer plays an important role in supplying carriers to the channel. Both enhanced carrier confinement and carrier increment allow a better modulation of the channel electrons by the gate voltage, which effectively improve transconductance linearity. Generally, the approaches to improve linearity usually generate undesirable features such as g_m and power gain reduction at high current levels [2]. However, by the combined action of the δ-doped layer and InGaN back barrier, the proposed DH-HEMT not only increases g_m and its corresponding power gain but also raises driving current.

II. Transistor Design

The proposed DH-HEMT structure with a gate length of

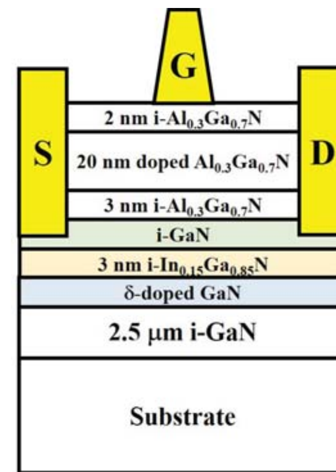

Fig.1 Schematic cross section of the proposed double-heterojunction HEMT.

0.3μm is schematically illustrated in fig.1, which is used in the following simulation. In fig.1, the channel region is composed of an undoped GaN channel, a 3-nm $In_{0.15}Ga_{0.85}N$ back barrier layer, and a 1-nm δ-doped layer with doping concentration of $5x10^{19}$ cm^{-3}.

Instead of being used as the major channel, the $In_{0.15}Ga_{0.85}N$ layer is inserted below the GaN channel. The 3-nm thickness and 15% Indium composition in the InGaN layer are designed to achieve two goals. (1) The conduction band offset and strain-induced polarization charge are 391meV and $1.39x10^{13}$ cm^{-2}, respectively. The strain-induced polarization field in the InGaN layer raises the conduction band profile of the GaN buffer, thus significantly enhancing the carrier confinement. (2) The thickness of the $In_{0.15}Ga_{0.85}N$ layer is designed as thin as 3-nm to reduce the risk of indium cluster formation [5]. In addition, Si δ-doping in a GaN layer is able to reach a sheet charge density as high as $1x10^{12}$ cm^{-2} to $2x10^{13}$ cm^{-2} [6]. Therefore, a δ-doped layer is designed to insert at the backside of the InGaN layer and is treated as a carrier supplier.

III. Model Calibration

It is clear that the polarization fields play a critical role in AlGaN/GaN HEMTs and are the primary source of the sheet charge density in the devices. Therefore, in order to model the sheet charge density correctly in the heterostructure under an applied gate voltage, the Poisson and Schrodinger equations are solved self-consistently at the heterojunction. The 3D free carriers and the partial neutralization of donors are directly taken into account in place of the usual assumption of fully ionized donors in the doped layer. Moreover, the polarization effects can be incorporated into the model by the boundary condition at the heterointerface. That is the electric displacement must be continuous at the heterointerface [7]. The field-dependent mobility in the GaN HEMT is obtained from an analytical formula extracted from Monte Carlo simulation [8]. The calculation of drain-current voltage characteristics is made using a quasi-two-

© 2020 The Japan Society of Applied Physics
Authorized licensed use limited to: Tsung-Hsing Yu. Downloaded on February 05,2021 at 15:35:11 UTC from IEEE Xplore. Restrictions apply.

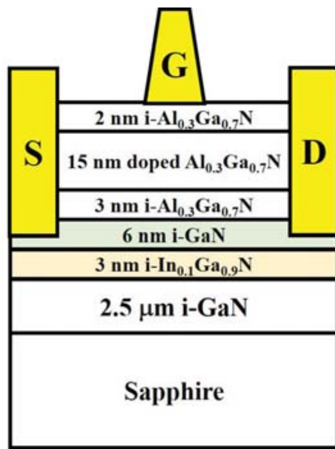

Fig.2 Schematic cross section of a GaN HEMT with a thin InGaN back barrier in ref [4] is used for model calibration.

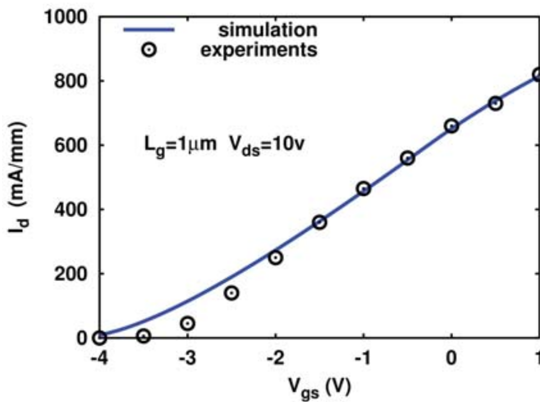

Fig.3 Comparison of I_d versus V_{gs} characteristics between simulation and measurements (symbols) for the $Al_{0.3}Ga_{0.7}N/GaN/In_{0.1}Ga_{0.9}N$ HEMT. The experimental data are from ref. [4].

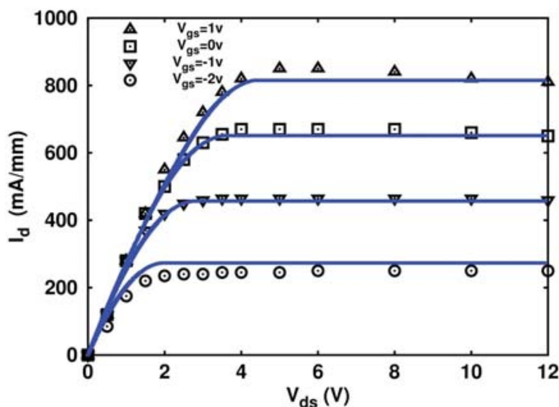

Fig.4 Calculated current-voltage characteristics (solid lines) compared to experimental data (symbols) at various gate biases for the $Al_{0.3}Ga_{0.7}N/GaN/In_{0.1}Ga_{0.9}N$ HEMT structure in ref.[4].

dimensional model [7] based on the self-consistent charge control and field-dependent mobility models.

To calibrate this model, a GaN HEMT with a thin $In_{0.1}Ga_{0.9}N$ back barrier structure [4] as schematically shown in fig.2 is used to simulate and compare to experiments. Excellent agreement between theory and experiments for both I_d-V_{gs} and I_d-V_{ds} characteristics is obtained over the full range of applied gate biases as can be seen from figs.3-4. The field-dependent mobility parameters and drain and source contact resistance are used to adjust to fit the measurements. The relevant polarization and material parameters are obtained from ref. [9].

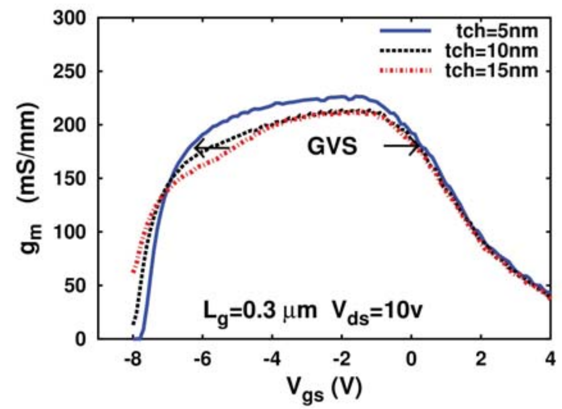

Fig.5 Calculated transconductance for $Al_{0.3}Ga_{0.7}N/GaN/In_{0.15}Ga_{0.85}N/\delta$-doped HEMTs under three different GaN channel thickness: tch=5nm,10nm, and 15nm.

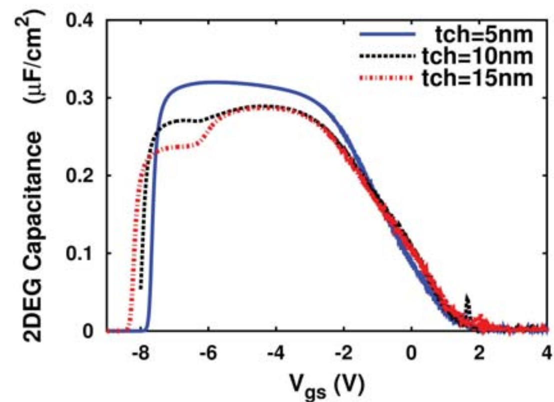

Fig.6 Calculated 2DEG capacitance under the gate in $Al_{0.3}Ga_{0.7}N/GaN/In_{0.15}Ga_{0.85}N/\delta$-doped HEMTs. As tch increases to 10nm and15nm, the minor channel formed in the InGaN layer leads to double-hump behavior.

IV. GaN Channel Thickness Optimization

Gate voltage swing (GVS) defined as the range of the gate voltage where the transconductance drops 80% of its peak value [6] is adopted to quantitatively measure the transconductance linearity. The channel thickness, tch, is defined as the distance between AlGaN and InGaN heterojunctions. Fig.5 plots the transconductance variations as the channel thickness, tch, increases from 5nm to 10nm and15nm. In fig.5, their corresponding GVS values decrease slightly from 6.6v to 5.8v. To further investigate the carrier dynamic behavior with respect to the gate voltage sweep in the channel, the calculated two-dimensional electron gas (2DEG) capacitance per unit area is visible in fig.6. The 2DEG capacitance is calculated by differentiating the sheet charge density under the gate with respect to the applied gate voltage. As the gate voltage increases, the capacitance increases quickly because of the band bending and an increase in the confined electrons induced by the gate voltage. Once the 2DEG is formed, the effective position of the 2DEG from the heterointerface is no longer noticeably influenced. Hence, the capacitance remains almost constant around the maximum capacitance.

However, the 2DEG capacitance in fig.6 clearly illustrates that there are two humps in the HEMTs with tch=10nm and tch=15nm. This is because two separated channel are formed in the GaN channel and InGaN layer, respectively. The major part of the channel is formed by the GaN channel between AlGaN and InGaN heterojunctions. The minor part of the channel is generated from the InGaN layer. This double-hump characteristics result from two separated

Authorized licensed use limited to: Tsung-Hsing Yu. Downloaded on February 05,2021 at 15:35:11 UTC from IEEE Xplore. Restrictions apply.

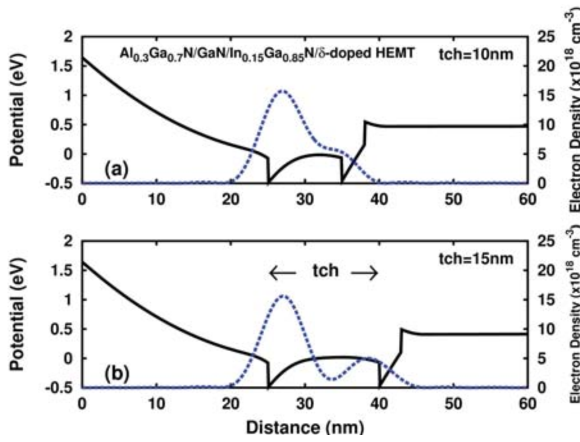

Fig.7 Conduction band profiles and electron density at a gate bias of zero voltage for GaN channel thickness (a) tch=10nm and (b) tch=15nm. The Fermi-level is set to zero.

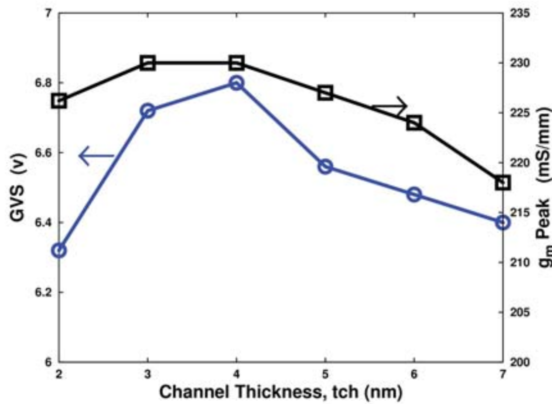

Fig.8 Channel thickness, tch varies from 2nm to 7nm and their corresponding GVS (circle symbols) and g_m peak (square symbols). With tch=4nm, a DH-HEMT has the highest GVS and g_m peak.

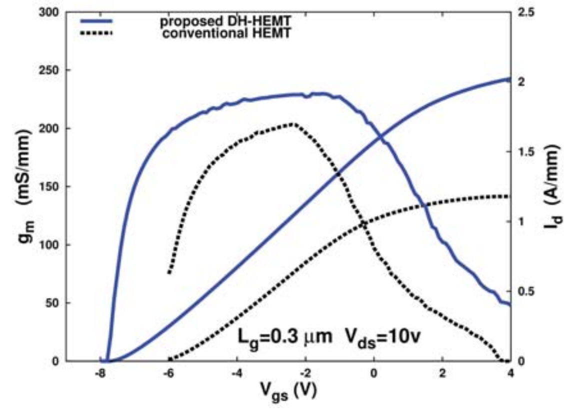

Fig.9 DC transfer characteristics comparison between the proposed DH-HEMT and a conventional HEMT. The proposed HEMT significantly improves linearity compared to the conventional one.

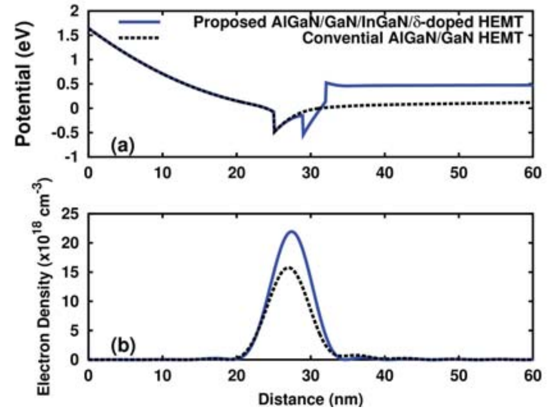

Fig.10 Two major features cause the linearity improvement in the proposed HEMT structure. (a) Raise the conduction band profile in the GaN buffer layer. (b) Increase electron density in the channel. The applied gate bias is 0v and the Fermi-level is set to zero.

channels and lead to a secondary transconductance peak that degrades the device's linearity [4][6]. Fig.7 gives the example of two separated channels from the self-consistent results of DH-HEMTs. The conduction band profile and confined carrier concentration are illustrated in fig.7(a) channel thickness tch=10nm and fig.7(b) tch=15nm, respectively. It is noted that the Fermi-level is set to a reference level and set equal to zero in fig.7. Also the applied gate bias is 0v. Fig.8 displays the channel thickness optimization results. It is observed that with tch=4nm, a DH-HEMT has the highest GVS and its corresponding g_m peak. As a result, a 4-nm thick GaN channel is employed in the following HEMT discussions.

V. Comparison between Proposed and Conventional HEMTs

A comparison of the dc transfer characteristics for the proposed HEMT and a conventional one is shown in fig.9. The drain-to-source voltage is biased at 10V. The maximum transconductance of 230 mS/mm in the proposed device with a Vgs=-1.8v is larger than that of 203 mS/mm in the conventional HEMT with a Vgs=-2.4v. The maximum g_m is influenced by two factors: capacitance due to 2DEG and low-field mobility. The 2DEG capacitance demonstrates how much charge can be supplied to the 2D channel with respect to a variation of the gate voltage. The excess supply charge directly contributes to an increase of the drain current. In addition to the modulation of charge in the 2D channel, the electrons in the channel are not all traveling at the saturated or peak electron velocity except those at the drain edges. Hence, g_m is also proportional to the low-field mobility. To simplify the calculation, the same magnitude of low-field mobility is assumed in fig.9 simulation. Therefore, the g_m in fig.9 indicates that the modulation efficiency of 2D channel charge is significantly improved in the proposed device. The maximum drain current of 2023 mA/mm at a gate bias of 4.0v and a drain bias of 10v in the proposed HEMT is 72% larger than that of the conventional device with the same bias.

As can be seen from fig.9, the proposed device's transconductance with respect to that in the conventional HEMT is quite flat and remains close to its peak value at high current levels. Their GVS values are 6.8v and 3.8v, respectively. The substantial linearity improvement results from two reasons: One, the carrier confinement is enhanced by the raised conduction band induced by the InGaN layer as evident from the fig.10(a). Two, the δ-doped layer significantly increases 2D carrier density in the channel as illustrated by fig.10(b).

VI. InGaN and Δ-doped Effects

Fig.11 reveals the calculated sheet carrier concentration as a function of gate voltage under three epilayer conditions: the proposed DH-HEMT, without δ-doped, and without InGaN layer structures, respectively. As the gate voltage increases, the free electrons in the 2D channel tend to go into the doped layer as 3D free electrons or to neutralize the donors. As a result, the sheet carrier concentration in the 2D channel becomes saturated, which limits the maximum

Authorized licensed use limited to: Tsung-Hsing Yu. Downloaded on February 05,2021 at 15:35:11 UTC from IEEE Xplore. Restrictions apply.

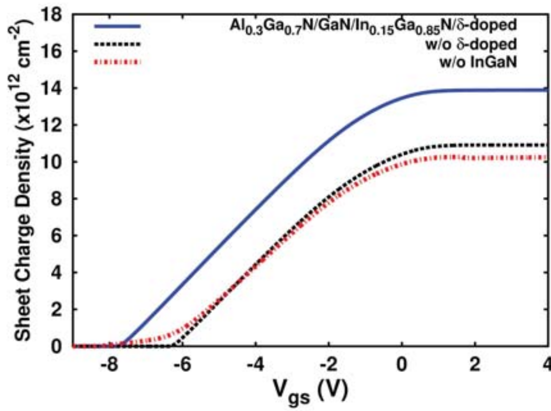

Fig.11 Calculated sheet charge density in 2D channel for a DH-HEMT under three different layer conditions: the proposed DH-HEMT, without δ-doped, and without $In_{0.15}Ga_{0.85}N$ layer structures.

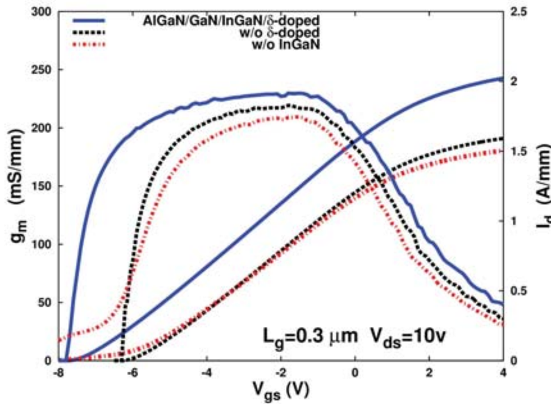

Fig.12 DC transfer characteristics for a DH-HEMT under three different layer conditions: the proposed DH-HEMT, without δ-doped, and without $In_{0.15}Ga_{0.85}N$ layer structures.

voltage swing in the HEMTs. The δ-doped layer in the proposed HEMT demonstrates a 29% of the sheet charge density increase compared to the HEMT without this layer at a gate bias of 0v in fig.11. Similarly, poor carrier confinement cannot sustain larger charge density in the channel as shown in the device without InGaN case. Therefore, the δ-doped layer, together with a thin InGaN layer, obtains a wide linear range of transconductance as can be seen from fig.12. Also, this wider linear range of transconductance results from the wider voltage swing in fig.11. Consequently, The effects of the carrier increment and enhanced carrier confinement act on the channel simultaneously to enlarge a wider voltage swing corresponding to the g_m linearity improvement.

In addition, the influence of AlGaN top barrier thickness on g_m is given in fig.13. Two top barrier thickness of 25nm and 18nm are examined in this plot. As the top barrier thickness decreases, the modulation of the 2D channel charge by the gate voltage is increased. Therefore, the g_m in 18nm thickness is higher than that in 25nm case. Hence, the AlGaN thickness can be optimized to obtain the best trade-off between power gain and linearity.

VII. Conclusions

This article presents a new DH-HEMT structure to improve transconductance linearity. The simulation model is well calibrated with the experiments indicating that the

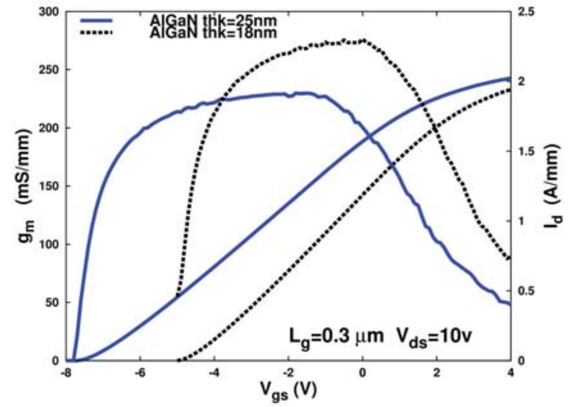

Fig.13 Top barrier AlGaN thickness impacts on DC transfer characteristics. Thinner top barrier thickness increases g_m but its corresponding GVS becomes small.

model can be successfully employed to project DH-HEMT performance. It is found that to maintain transconductance linearity at high current levels, the conducting channel needs to sustain sufficient larger 2D charge. This can be achieved by using the InGaN and δ-doped layers together to enhance carrier confinement and increase carrier density in the channel. These two factors result in a larger sheet charge in the channel. To deplete this larger sheet charge at the heterointerface, the threshold voltage in the HEMT device becomes more negative, corresponding to a larger voltage swing. Moreover, compared to the conventional HEMT, the transconductance in the proposed device decreases slowly as the gate voltage switches to a forward bias. This also indicates that the proposed DH-HEMT can be employed in a larger voltage swing. Consequently, the proposed DH-HEMT exhibits the potential for high power and high frequency applications.

References

[1] S. Bajaj, Z. Yang, F. Akyol, P. S. Park, Y. Zhang, A. L. Price, S. Krishnamoorthy, D. J. Meyer, and S. Rajan, "Graded AlGaN Channel Transistors for Improved Current and Power Gain Linearity," IEEE Trans. Electron Devices, vol. 64, no. 8, pp. 3114-3119, Aug. 2017.

[2] J. Liu, Y. Zhou, R. Chu, Y. Cai, K. J. Chen, and K. M. Lau, "Highly Linear $Al_{0.3}Ga_{0.7}N$-$Al_{0.05}Ga_{0.95}N$-GaN Composite-Channel HEMTs," IEEE Electron Device Lett., vol. 26, no. 3, pp. 145-147, Mar. 2005.

[3] T. Palacios, A. Chakraborty, S. Heikman, S. Keller, S. P DenBaars, and U. K. Mishra, "AlGaN/GaN High Electron Mobility Transistors with InGaN Back-Barriers," IEEE Electron Device Lett., vol. 27, no. 1, pp. 13-15, Jan. 2006.

[4] J. Liu, Y. Zhou, J. Zhu, Y. Cai, K. M. Lau, and K. J. Chen, "DC and RF Characteristics of AlGaN/GaN/InGaN/GaN Double-Heterojunction HEMTs," IEEE Trans. Electron Devices, vol. 54, no. 1, pp. 2-9, Jan. 2007.

[5] J. Liu, Y. Zhou, J. Zhu, K. M. Lau, and K. J. Chen, "AlGaN/GaN/InGaN/GaN DH-HEMTs with an InGaN Notch for Enhanced Carrier Confinement," IEEE Electron Device Lett., vol. 27, no. 1, pp. 10-12, Jan. 2006.

[6] C. Tang, K. H. Teo, and J. Shi, "Simulation of GaN HEMT with Wide-Linear-Range Transconductance," in Proc. Electron Device and Solid-State Circuit Conference, 2017

[7] T.-H. Yu and K. F. Brennan, "Theoretical Study of a GaN-AlGaN High Electron Mobility Transistor Including a Nonlinear Polarization Model," IEEE Trans. Electron Devices, vol. 50, no. 2, pp. 315-323, Feb. 2003.

[8] T.-H. Yu and K. F. Brennan, "Monte Carlo Calculation of Two-dimensional Electron Dynamics in GaN-AlGaN Heterostructures," J. Appl. Phys., vol. 91, pp. 3730-3736, Mar. 2002.

[9] C. Wood and D. Jena, *Polarization Effects in Semiconductors*, Springer, 2008

Authorized licensed use limited to: Tsung-Hsing Yu. Downloaded on February 05,2021 at 15:35:11 UTC from IEEE Xplore. Restrictions apply.